Electronic Supplementary Material (ESI) for Organic & Biomolecular Chemistry
This journal is © The Royal Society of Chemistry 2022

Electronic supplementary information

Synergestic enhancement of antibacterial effect by a supramolecular strategy

Mengke Ma,‡[ab] Junyi Chen,‡[b] Yahan Zhang,[b] Xingbei Du,[b] Longming Chen,[b] Xiang Yu,[b] Zhengui Zhou,*[c] Yang Liu,*[a] Qingbin Meng*[ab]

[a] Key Laboratory of Structure-Based Drug Design & Discovery of the Ministry of Education, Shenyang Pharmaceutical University, Shenyang 110016, China. E-mail: y.liu@syphu.edu.cn

[b] State Key Laboratory of Toxicology and Medical Countermeasures, Beijing Institute of Pharmacology and Toxicology, Beijing 100850, P. R. China. E-mail: nankaimqb@sina.com

[c] Gongan County People's Hospital, Jingzhou 434399, P. R. China, E-mail: zzg750@126.com

Table of Contents

1 General materials and methods S2

1.1 Materials S2

1.2 Instruments S2

1.3 Cell, bacterial strains and animal S2

1.4 Fluorescence titration S3

1.5 Cytotoxicity assay S3

1.6 Inhibition of biofilm and bacterial experiments S3

1.7 *In vivo* synergetic antibacterial effect S4

2 Synthetic route of WP5A S5

3 Supporting results and experimental raw data S7

3.1 ^{1}H-ROESY NMR spectra for complexation of AzA with WP5A. S7

3.2 Job's plot analysis for complexation of WP5A with AzA S7

3.3 Optimized geometries for host-guest complex of AzA/WP5A. S8

3.4 Determination of inhibiting biofilm activity S8

3.5 *In vitro* cytotoxicity assay of WP5A S10

3.6 Body weight change of mice after exposure to WP5A S11

3.7 H&E staining for major organs S11

3.8 *In vivo* synergetic anti-infective effect S12

References S13

1. General materials and methods

1.1 Materials. All agents were purchased commercially and used without further purification unless otherwise noted. Dulbecco's modified eagle medium (DMEM) was purchased from Gibco (Thermo Fisher Scientific). Fetal bovine serum (FBS), penicillin-streptomycin and PBS were purchased from Invitrogen (Carlsbad, CA, USA). The cell counting kit-8 (CCK-8) was purchased from Dojindo China Co. Ltd. (Shanghai, China). Bacterial strain *S. aureus* (ATCC 25923) were purchased from Shanghai Fuxiang Biotechnology Co. Ltd (Shanghai, China).

1.2 Instruments. ^{1}H NMR spectra was recorded at Bruker Advance 600 MHz. Fluorescence spectroscopic studies were carried out by a FL-6500 fluorescence spectrophotometer, PerkinElmer Co. Ltd. Fluorescence imaging were recorded by IVIS Spectrum system, PerkinElmer, Inc. Cytotoxicity studies were performed on SpectraMax ® M5 plate reader, Molecular Devices. etry (MALDI-TOF mass spectrometry) were examined on a BrukerReex mass spectrograph.

1.3 Cell, bacterial strains and animal. The human immortalized keratinocytes (HaCaT) cells were purchased from the cell bank of Chinese Academy of Science. HaCaT cells were cultured in DMEM supplemented with 10% FBS, 1% penicillin and 1% streptomycin. Then cells were incubated at 37 ℃ under 5% CO_2 and 90% relative humidity, and passaged every 2 days.

S. aureus was maintained in 80 % sterile glycerol at -80 ℃. After being thawed, the aliquots were diluted (1 : 2000) in fresh sterile broth and grown overnight at 37 ℃ with agitation.

Six-week-old kunming mice (~20 g body weight) were purchased from SPF Biotechnology Co., Ltd. (Beijing, China) and maintained at 25 ℃ in a 12 h light/dark cycle with free access to food and water. Animals were allowed to acclimate to environment for at least one week before experiments. All experimental procedures were conducted in accordance with the Guide for the Care and Use of Laboratory Animals of the AAALAC, and were approved by the Animal Care and Use Committee of the National Beijing Center for Drug Safety Evaluation and Research. Best efforts

were made to minimize the number of animals used and their suffering.

1.4 Fluorescence titration. To quantitatively assess the complexation behavior of these compounds, fluorescence titrations of hosts with guests were performed at 298 K in a 10 mM PBS of pH 7.4. The complexation of the host and the guest was measured according to the procedure reported previously.[1]

1.5 *In vitro* cytotoxicity studies. The relative cytotoxicity of WP5A against HaCaT cells was accessed in vitro by using CCK-8 assays. HaCaT cells were seeded into 96-well plates at a density of 8000 cells per well in 100 μL of DMEM supplemented with 10% FBS, 1% penicillin, and 1% streptomycin. Then added WP5A to the cell-containing wells which were further incubated at 37 ℃under 5% CO_2 for 72 h. After rinsing by PBS buffer, 10 μL of CCK-8 was added into each well and incubated for another 0.5 h. Using plate reader to measure plate at 450 nm. Each concentration of compound was tested in five wells.[1]

1.6 Inhibition of biofilm and bacterial experiments. Analysis of biofilm inhibition: WP5A, AzA and 1:1 mixture of AzA/WP5A were dissolved in the sterile broth, and 100 μL of sample solution was subjected to two-fold serial dilution in sterile broth in 96-well plates, added to 10 μL of the bacterial suspension, and incubated at 37 ℃ for 24 h to establish biofilm. Turn over the plates and rinse vigorously three times with doubly distilled water. Next, 0.4% crystal violet (200 μL) was added to each well for 45 min. After vigorously rinsing three times with DDW, 200 μL of 33% acetic acid is added to each well. The plate was shaken for 15 min to release the dye. The absorbance of appropriate blank well at 600 nm use a plate reader. Each concentration of compound was tested in five replicates, and three independent experiments were performed.

Antibacterial activity: The antibacterial activities of samples were determined in sterile 96-well plates by the broth microdilution method. The bacterial strains were incubated with shaking at 170 rpm in 4 mL of the sterile broth at 37 ℃. After overnight incubation, the concentration of bacteria reached 1×10^9 CFU·mL^{-1}. Then bacterial suspensions were diluted (1:2000, approximately 2×10^5 CFU·mL^{-1}) and incubated with different concentration of samples in sterile 96-well plates at 37 ℃ for 24 h. The MIC is defined as the lowest concentration of testing chemical that inhibits visible growth of

bacteria as observed with the unaided eye.[3]

1.7 *In vivo* synergetic antibacterial effect. Six-week-old kunming mice (~ 20 g body weight) were used. Four mice without any infection were set as normal group, and all the other mice infected by *S. aureus* were randomly divided into four groups (n = 4): (1) PBS; (2) AzA; (3) WP5A; (4) AzA/WP5A. The mice were anaesthetized, depilated and the 7 mm diameter full-thickness excisional wounds were inflicted on the dorsal skin as described. Next, bacteria (*S. aureus*, 1×10^5 CFU in 20 μL of PBS) were topically inoculated into the wounds. After 24 h infection, 50 μL of AzA (1 mM), WP5A (1 mM), AzA/WP5A (1 mM) solution was dropped on the wound area. The group with PBS treatment served as the control. All the therapy procedures were administered once at 8 a.m. every other day, and the whole experimental time was nine days. To record the process of wound healing and weight body, the size of wound was measured by a caliper and photographed. In addition, on the 9th day, the wound tissues of the mice were homogenized with sterile PBS and diluted with an appropriate dilution factor, and the amount of the bacteria in the wound was determined by using spread plate method. In addition, the skin of another mice was cut and fixed in 4% paraformaldehyde solution for H&E and immunohistochemistry staining to evaluate the potential side effects.

2 Synthetic route of WP5A

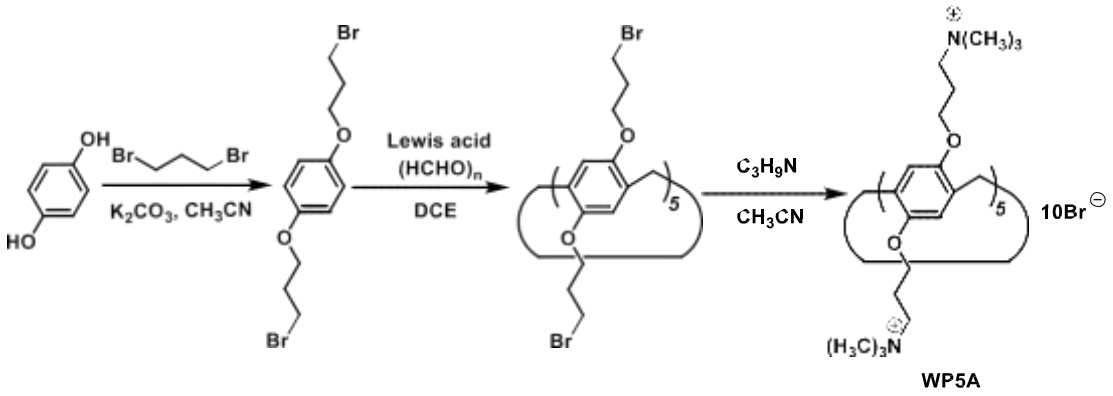

Scheme 1. Synthetic route of WP5A.

WP5A was synthesized and purified according to the procedure reported previously.[4]

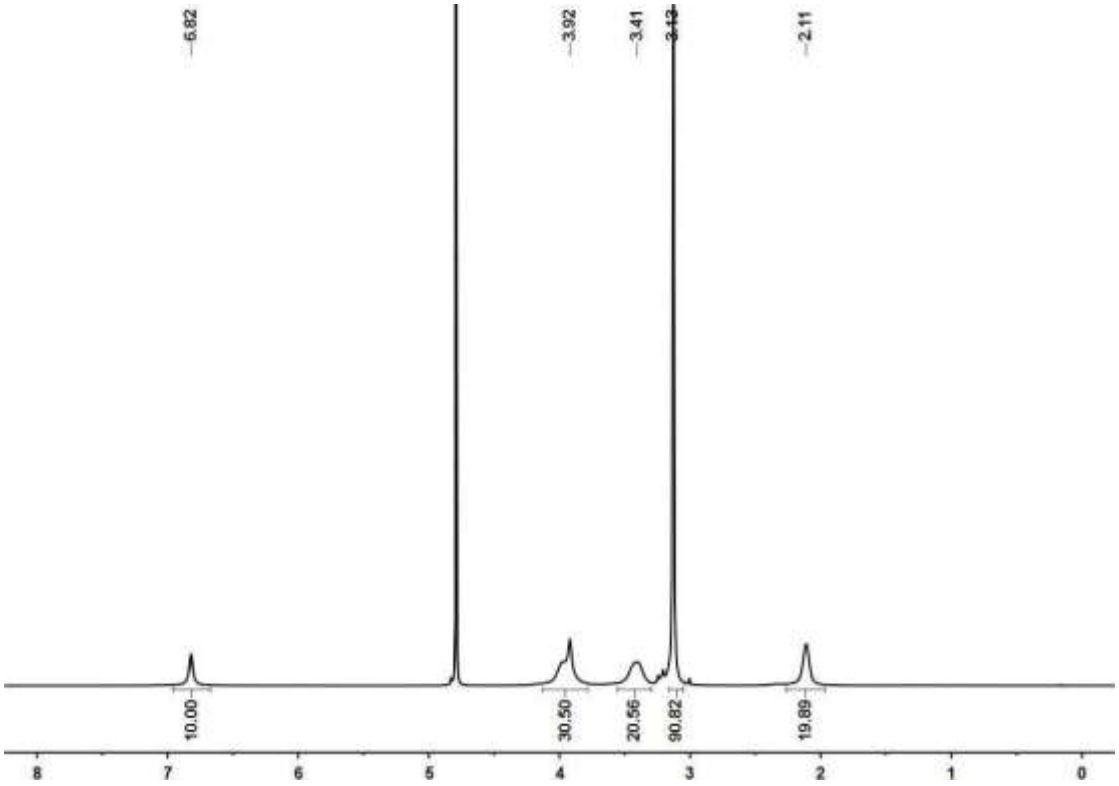

Fig. S1. ^{1}H NMR spectrum of WP5A in D_2O, 600 MHz.

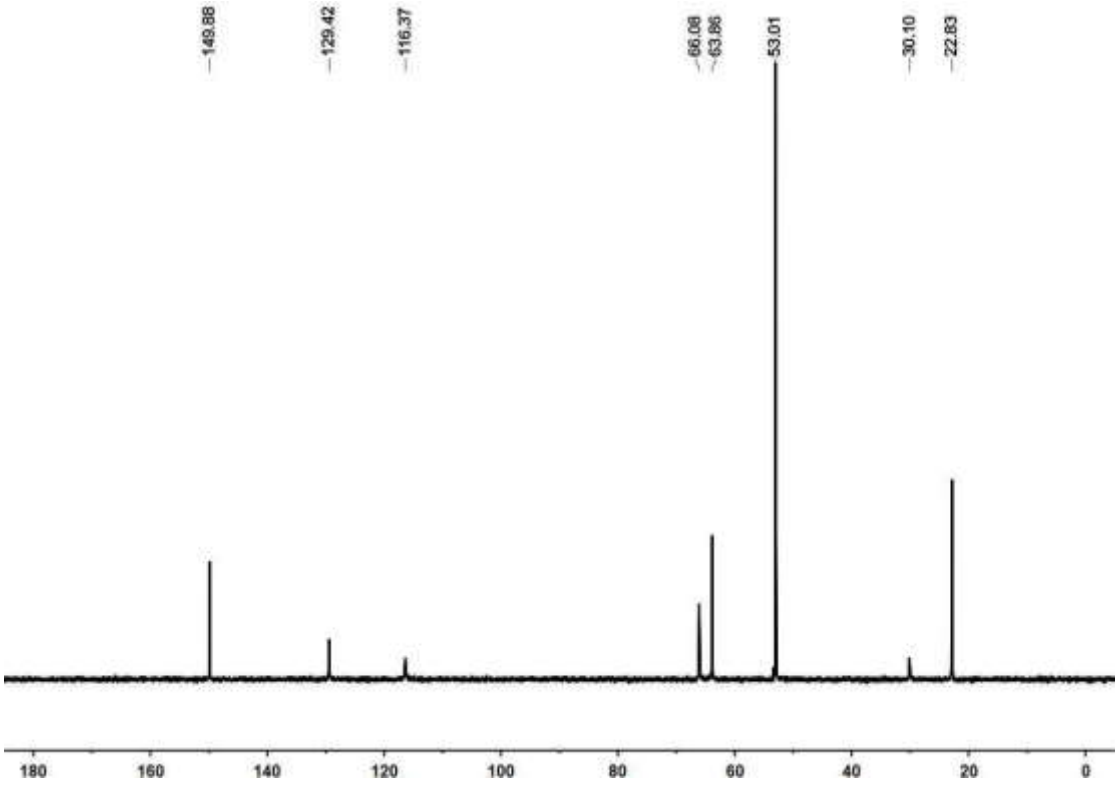

Fig. S2. ^{13}C NMR spectrum of WP5A in D_2O, 150 MHz.

3 Supporting results and experimental raw data

3.1 ^{1}H-ROESY NMR spectra for complexation of AzA with WP5A.

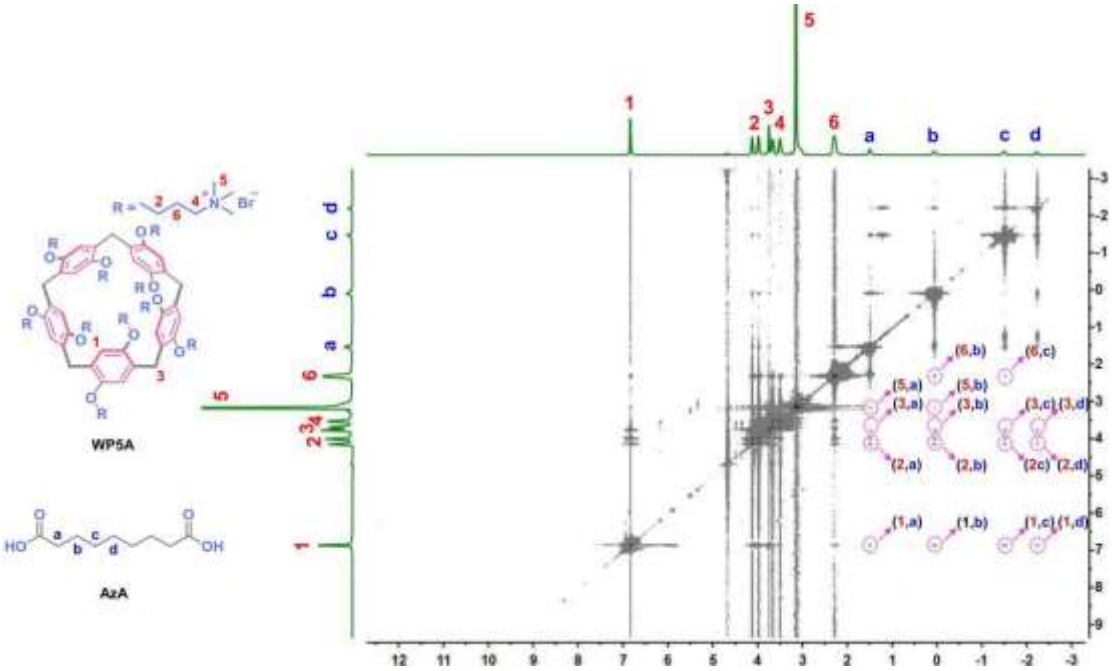

Fig. S3. ^{1}H-ROESY NMR spectra (600 MHz, D_2O, 2.0 mM) for complexation of AzA with WP5A.

3.2 Job's plot analysis for complexation of AzA with WP5A.

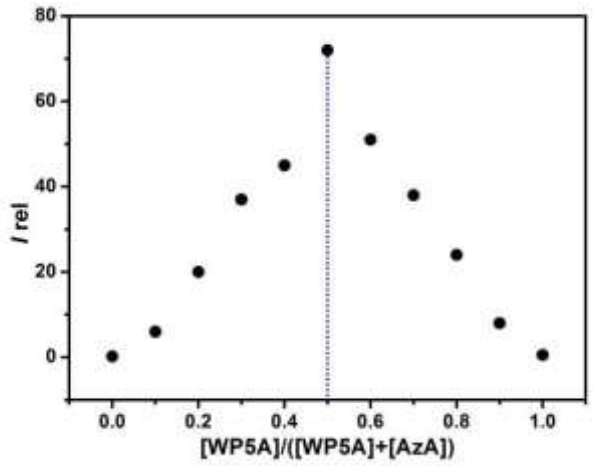

Fig. S4. Job's plot for WP5A with AzA in 10 mM PBS buffer at pH 7.4 (λ_{ex} = 290 nm, λ_{em} = 328 nm, [AzA] + [WP5A] = 1.0 mM).

3.3 Optimized geometries for host-guest complex of AzA/WP5A.

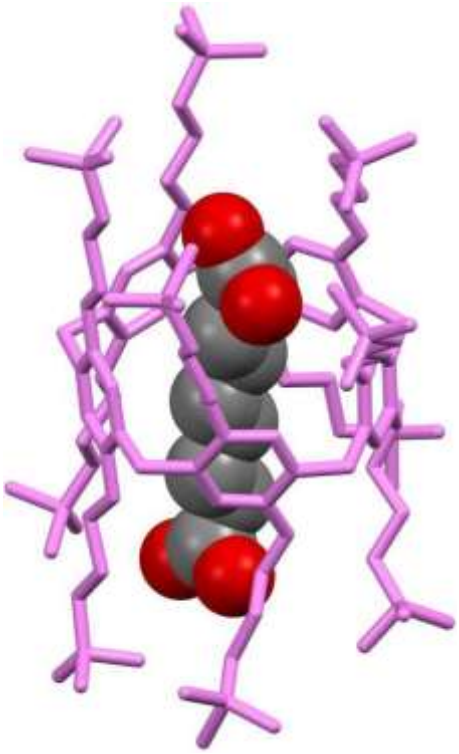

Fig. S5. The optimized geometrie structure of the MM2 energy-minimized model of the AzA/WP5A complex.

3.4 Determination of inhibiting biofilm activity.

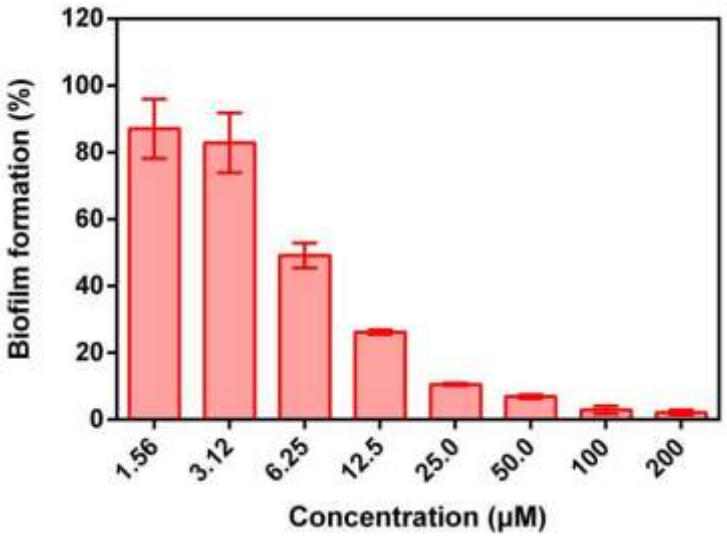

Fig. S6. Inhibition of biofilms assay by increasing concentration of WP5A. (mean ± SD, n = 5).

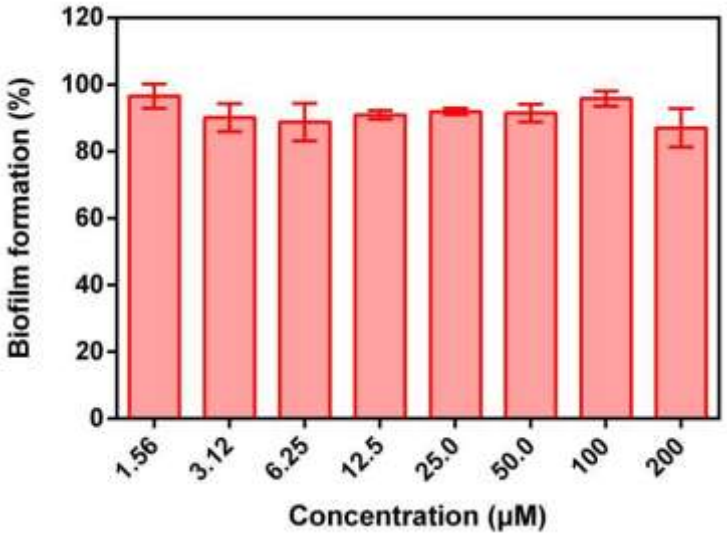

Fig. S7. Inhibition of biofilms assay by increasing concentration of AzA. (mean ± SD, n = 5).

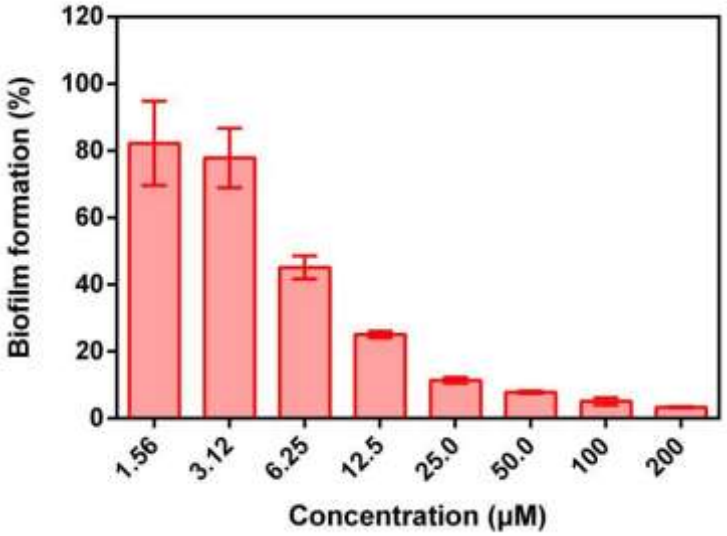

Fig. S8. Inhibition of biofilms assay by increasing concentration of AzA/WP5A. (mean ± SD, n = 5).

3.5 *In vitro* cytotoxicity assay of WP5A.

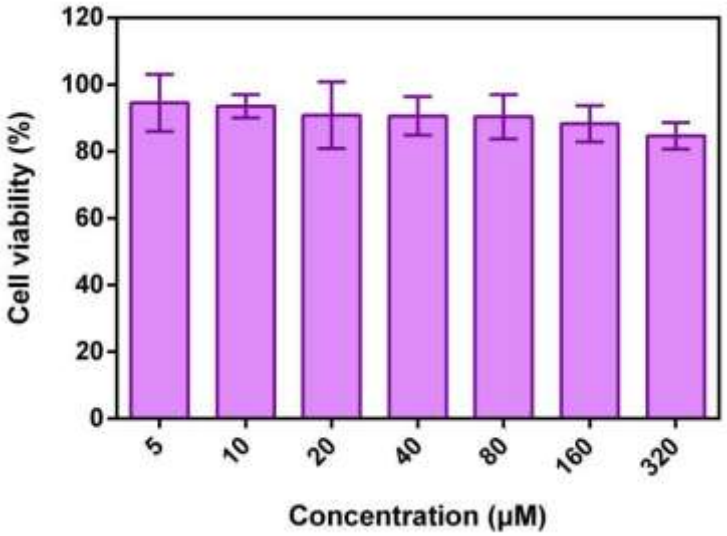

Fig. S9. Relative cell viabilities of HaCat cell after incubation for 72 h with WP5A at the indicated concentrations. Cell death was then measured by using a CCK-8 assay (mean ± SD, n = 5).

3.6 Body weight change of mice after exposure to WP5A.

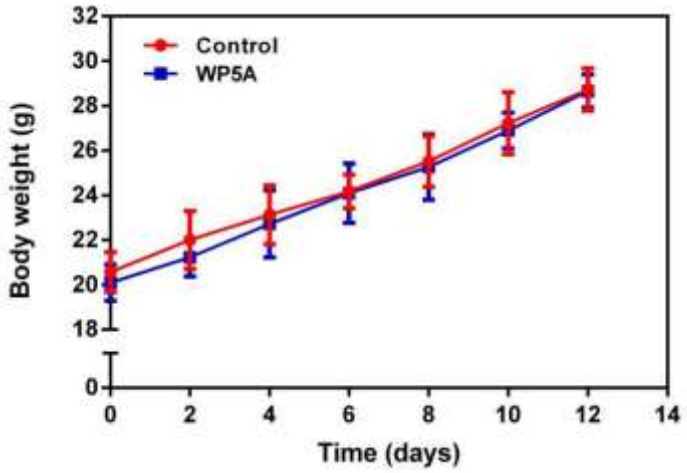

Fig. S10. Change in body weight of mice after exposure to WP5A (50 μM, two-day administration in a row) compared with the control group. Data were represented as mean ± SD, n = 4. This was no statistically significant difference in body change between WP5A and control groups over a period of 12 days.

3.7 H&E staining for major organs.

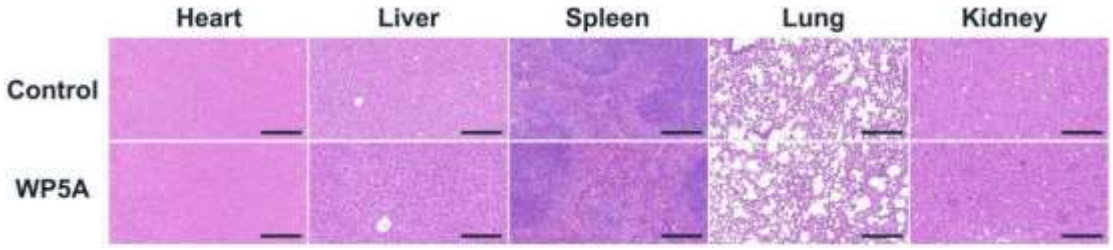

Fig. S11. H&E stains of the major organs from mice after exposure to WP5A compared with normal group (scale bar: 50 μm).

3.8 *In vivo* synergetic anti-infective effect.

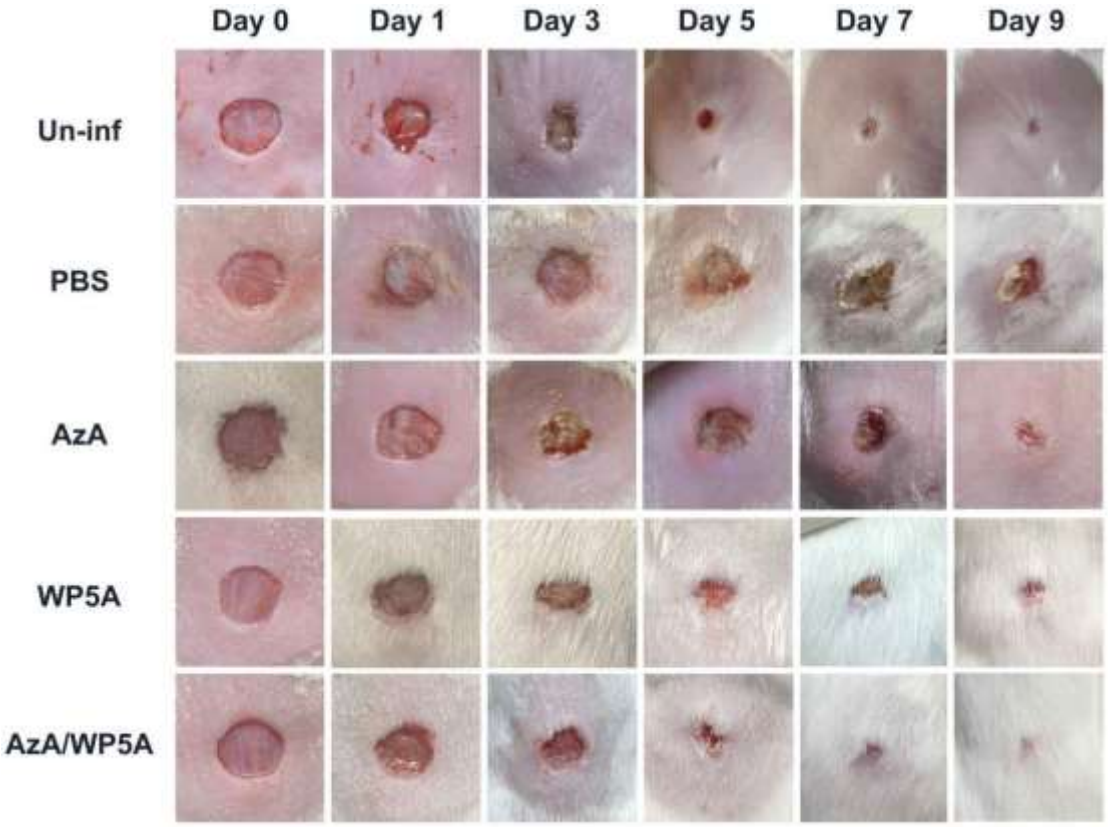

Fig. S12. Representative images of wound changes after treatment with 50 μL of AzA (1 mM), WP5A (1 mM) and AzA/WP5A (1 mM) within 9 days. The Un-inf group represents uninfected skin wounds.

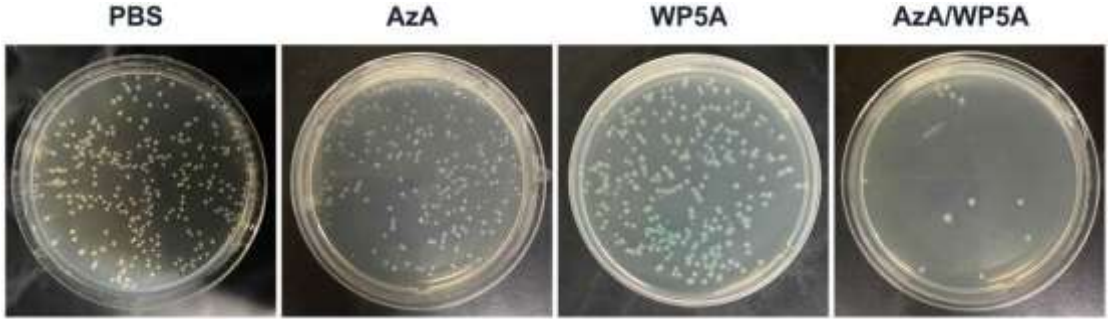

Fig. S13. Evaluation of bacterial colonies inside the infected skin after treatment.

References

(1) J. Chen, Y. Zhang, Z. Meng, L. Guo, X. Yuan, Y. Zhang, Y. Chai, J. L. Sessler, Q. Meng, C. Li, *Chem. Sci*., **2020**, *11*, 6275-6282.

(2) J. Chen, Y. Zhang, Y. Chai, Z. Meng, Y. Zhang, L. Chen, D. Quan, Y. Wang, Q. Meng, C. Li, *Chem. Sci.*, **2021**, *11*, 5202-5208.

(3) I. Wiegand, K. Hilpert, R. E. W. Hancock, *Nature Proto*., **2008**, *3*, 163-175.

(4) R. Joseph, A. Naugolny, M. Feldman, I. M. Herzog, M. Fridman, Y. Cohen, *J. Am. Chem. Soc*., **2016**, *138*, 754-757.